




## ARTICLE

# Microwave ablation of primary breast cancer inhibits metastatic progression in model mice via activation of natural killer cells

Muxin Yu<sup>1,2</sup>, Hong Pan<sup>1,2</sup>, Nan Che<sup>3</sup>, Li Li<sup>1,2,4</sup>, Cong Wang<sup>5</sup>, Yue Wang<sup>1,2</sup>, Ge Ma<sup>1,2</sup>, Mengjia Qian<sup>1,2</sup>, Jiawei Liu<sup>1,2</sup>, Mingjie Zheng<sup>1</sup>, Hui Xie<sup>1</sup>, Lijun Ling<sup>1</sup>, Yi Zhao<sup>1</sup>, Xiaoxiang Guan<sup>6</sup>, Qiang Ding<sup>1,2</sup>, Wenbin Zhou<sup>1,2</sup>  and Shui Wang<sup>1,2</sup>

Surgery is essential for controlling the symptoms and complications of stage IV breast cancer. However, locoregional treatment of primary tumors often results in distant progression, including lung metastasis, the most common type of visceral metastasis. As a minimally invasive thermal therapy, microwave ablation (MWA) has been attempted in the treatment of breast cancer, but the innate immune response after MWA has not yet been reported. Using two murine models of stage IV breast cancer, we found that MWA of primary breast cancer inhibited the progression of lung metastasis and improved survival. NK cells were activated after MWA of the primary tumor and exhibited enhanced cytotoxic functions, and the cytotoxic pathways of NK cells were activated. Depletion experiments showed that NK cells but not CD4<sup>+</sup> or CD8<sup>+</sup> T cells played a pivotal role in prolonging survival. Then, we found that compared with surgery or control treatment, MWA of the primary tumor induced completely different NK-cell-related cytokine profiles. Macrophages were activated after MWA of the primary tumor and produced IL-15 that activated NK cells to inhibit the progression of metastasis. In addition, MWA of human breast cancer stimulated an autologous NK-cell response. These results demonstrate that MWA of the primary tumor in metastatic breast cancer inhibits metastatic progression via the macrophage/IL-15/NK-cell axis. MWA of the primary tumor may be a promising treatment strategy for de novo stage IV breast cancer, although further substantiation is essential for clinical testing.

**Keywords:** breast cancer; microwave ablation; metastasis; NK cells; surgery

*Cellular & Molecular Immunology* (2021) 18:2153–2164; <https://doi.org/10.1038/s41423-020-0449-0>

## INTRODUCTION

De novo stage IV breast cancer is an incurable disease, and systemic therapy is used as the primary treatment to prolong survival. Typically, locoregional surgery is recommended to avert potential physical and/or mental symptoms and complications, such as fungation and bleeding. Primary tumor surgery improves survival by decreasing the tumor burden and removing the “seed source” of new metastases and drug-resistant clones, as demonstrated by several retrospective studies.<sup>1,2</sup> However, this survival benefit has not yet been observed in other retrospective studies that controlled potential biases.<sup>1,2</sup> Two randomized trials<sup>3,4</sup> considered the selection bias of retrospective studies and suggest that locoregional surgery on the primary tumor does not improve the overall survival of patients with de novo stage IV breast cancer, with a median follow-up of ~3 years. Strikingly, locoregional surgery had a significant detrimental effect on distant progression-free survival in both trials, especially in relation to visceral metastases,

including the most common type of metastasis, lung metastasis. Moreover, accumulating evidence suggests that surgical removal of the primary tumor increases metastatic spread.<sup>5–10</sup> The underlying mechanisms<sup>4,10</sup> involve the generation of a permissive environment for tumor growth<sup>9</sup> and direct alteration of neoplastic properties.<sup>8</sup> This phenomenon has been observed in other types of tumors, including testicular cancer and metastatic lung tumors.<sup>11–13</sup> Therefore, the local control of de novo stage IV breast cancer seems to be an intractable problem.

Minimally invasive thermal ablation of solid tumors has become a common practice, and weak innate and adaptive immune responses have been reported after thermal ablation of different types of tumors.<sup>14–19</sup> A previous study<sup>18</sup> inferred that the immune response may contribute to the unexplained, spontaneous regression of untreated distant metastases after radiofrequency ablation or cryosurgery in primary renal cell carcinoma or prostatic cancer in rare cases.<sup>20–22</sup> After thermal

<sup>1</sup>Department of Breast Surgery, The First Affiliated Hospital of Nanjing Medical University, 300 Guangzhou Road, Nanjing 210029, China; <sup>2</sup>Jiangsu Key Lab of Cancer Biomarkers, Prevention and Treatment, Jiangsu Collaborative Innovation Center For Cancer Personalized Medicine, School of Public Health, Nanjing Medical University, Nanjing 211166, China; <sup>3</sup>Department of Rheumatology and Immunology, The First Affiliated Hospital of Nanjing Medical University, 300 Guangzhou Road, Nanjing 210029, China; <sup>4</sup>Department of General Surgery, Huashan Hospital, Fudan University, Shanghai 200040, China; <sup>5</sup>Department of Pathology, The First Affiliated Hospital of Nanjing Medical University, 300 Guangzhou Road, Nanjing 210029, China and <sup>6</sup>Department of Oncology, The First Affiliated Hospital of Nanjing Medical University, 300 Guangzhou Road, Nanjing 210029, China  
Correspondence: Wenbin Zhou (zhouwenbin@njmu.edu.cn) or Shui Wang (ws0801@hotmail.com)

These authors contributed equally: Muxin Yu, Hong Pan, Nan Che, Li Li

Received: 4 March 2020 Accepted: 14 April 2020

Published online: 8 May 2020

ablation, T cells and antigen-presenting cells, including dendritic cells and macrophages, are activated. In addition, several cytokines, such as interleukin (IL)-1, IL-6, IL-10, and tumor necrosis factor (TNF)- $\alpha$ , are involved in the immune response.<sup>18</sup> Currently, this technique is being increasingly evaluated for breast cancer in several studies.<sup>23–27</sup> Due to several advantages over other thermal therapies,<sup>28,29</sup> including higher temperatures, larger ablation volumes, and shorter ablation times, microwave ablation (MWA) has been attempted in the treatment of breast cancer,<sup>23,30</sup> as it was found to induce a weak T-cell response in a murine model of breast cancer.<sup>31,32</sup> To the best of our knowledge, the natural killer (NK) cell response has seldom been evaluated after thermal ablation,<sup>15,16,33</sup> and that after MWA has not yet been reported. Moreover, the potential effect of the immune response on metastasis after MWA of the primary breast tumor has not been clarified.

Herein, we used two murine models of stage IV breast cancer and found that MWA of the primary breast cancer tumor inhibited the progression of lung metastasis and improved survival by activating NK cells. Moreover, macrophages/IL-15/NK cells constituted the key pathway involved in this abscopal effect. We also demonstrated that MWA of human breast cancer stimulated the autologous NK-cell response clinically. Therefore, MWA of the primary tumor may be a promising treatment strategy for de novo stage IV breast cancer, although further substantiation is essential for clinical testing.

## RESULTS

### MWA of primary breast cancer inhibits lung metastasis

To mimic clinical stage IV breast cancer, a BALB/c mouse-derived transplantable 4T1 tumor model was established. This model of metastatic cancer exhibits characteristics of human breast cancer.<sup>34</sup> BALB/c mice developed disseminated metastases within 10–21 days after 4T1 cell inoculation,<sup>34,35</sup> and the primary 4T1 tumor with lung metastases was treated at 28 days after inoculation (Fig. 1a). To exclude the nonspecific effects of MWA and surgery, sham surgery and MWA were performed on the left leg (sham MWA) in the same model (Fig. S1a). The number of pulmonary metastases in the sham surgery and sham MWA groups was similar to that in the control group at 7 days after treatment (Fig. S1b). Survival was prolonged in MWA-treated mice but not in the surgery group mice compared with the control group mice (Fig. 1b). The number of pulmonary metastases in the MWA group was lower than that in the surgery and control groups at 7 and 14 days after treatment (Fig. 1c), and the sizes of metastatic tumors seemed to be smaller on day 14 after MWA (Fig. 1d).

The effects of treatments on pulmonary metastases were investigated further. Apoptosis in pulmonary metastases was assessed using caspase 3 (Fig. 1e), and angiogenic activity was assessed using VEGF (Fig. 1f). We found that the VEGF level in pulmonary metastases was lower and that of caspase 3 was higher in the MWA group than in the surgery and control groups on days 7 and 14 after treatment. In addition, MWA of the primary tumor

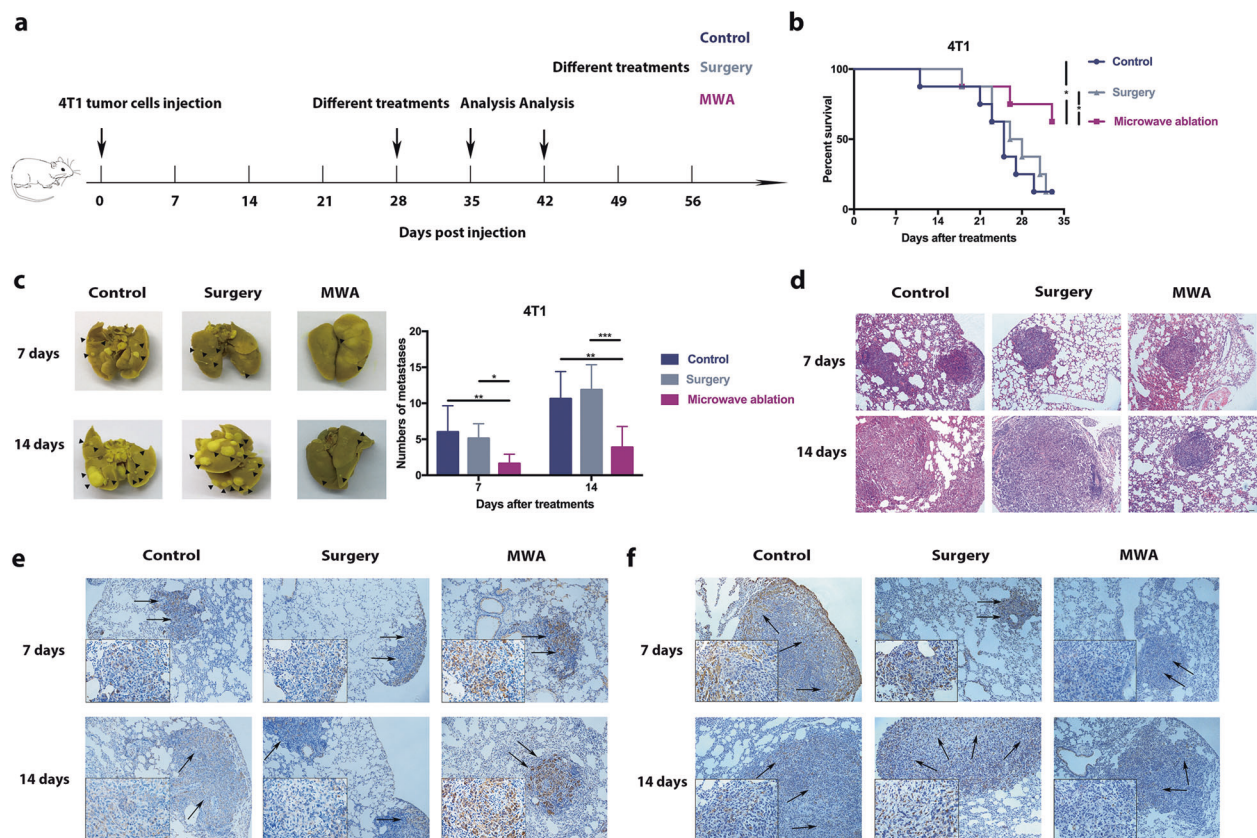


**Fig. 1** Microwave ablation (MWA) of primary breast tumors inhibited lung metastasis progression and improved survival in a BALB/c mouse-derived transplantable 4T1 tumor model. **a** Schematic illustration of the experimental design for **b–f**. **b** Primary 4T1 tumors were treated by MWA or surgery or received no treatment. Survival was analyzed using the log-rank test ( $*P < 0.05$ ). Compared with those in the no treatment and surgery groups, the mice in the MWA-treated group showed better survival ( $n = 8$  mice for each group). **c** Representative picture of lung lobes and the number of 4T1 lung metastases in mice that received MWA, surgery, or no treatment on days 7 and 14 after treatment. Numerical data are reported as the mean  $\pm$  SD. The significance of differences among the groups was assessed by a parametric test ( $*P < 0.05$ ;  $**P < 0.01$ ;  $***P < 0.001$ ). **d** HE staining of lung lobes collected from mice that received MWA, surgery or no treatment on day 7 or 14 after treatment. IHC staining for caspase 3 (**e**) and VEGF (**f**) in 4T1 lung metastases in the three groups 7 and 14 days after treatment. Scale bars, 50  $\mu$ m

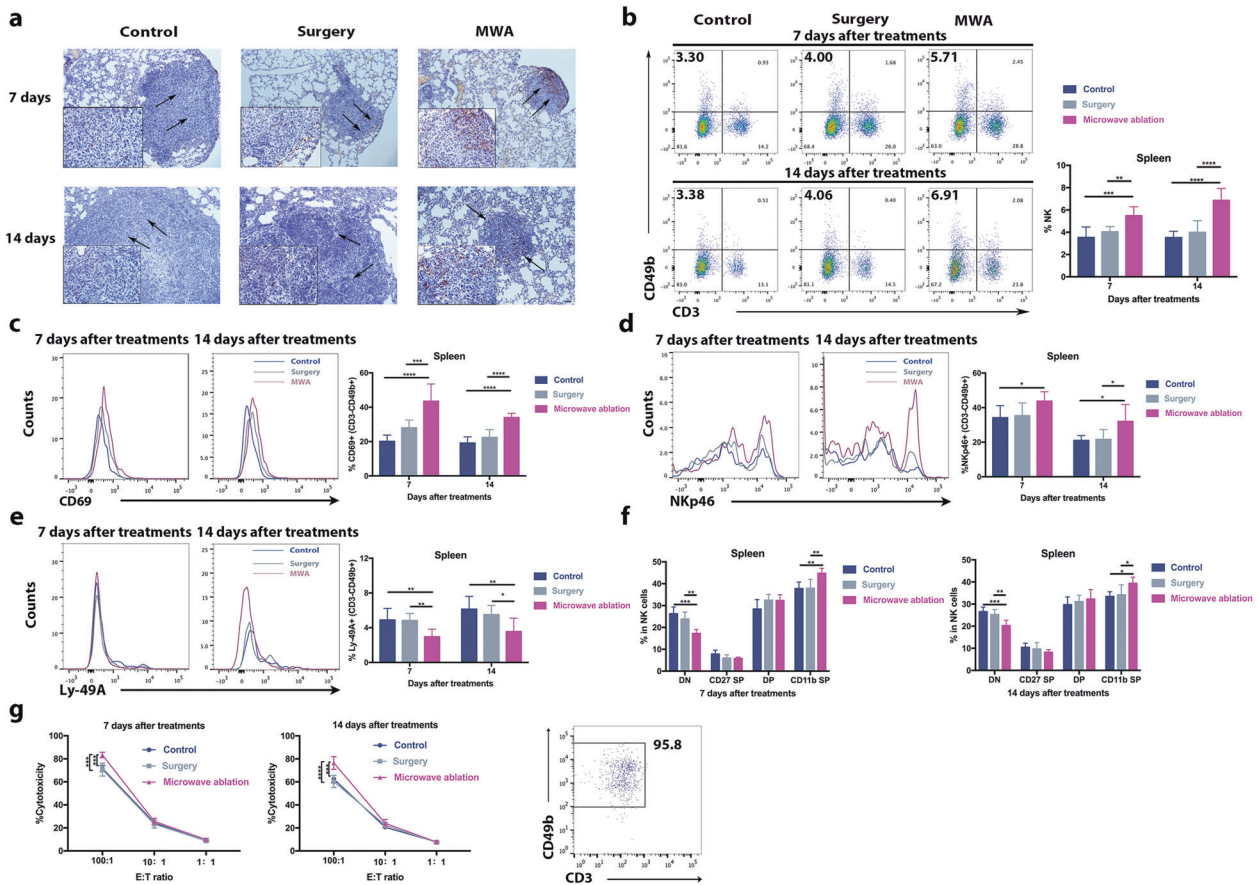


**Fig. 2** NK cells were activated after microwave ablation of primary breast cancer in a BALB/c mouse-derived transplantable 4T1 tumor model. **a** Infiltrated NK cells in the lung metastases of mice in different groups 7 or 14 days after treatment. Scale bars, 50  $\mu$ m. The percentages of splenic NK cells (**b**), CD69+ NK cells (**c**), NKp46-positive NK cells (**d**), and Ly-49A-positive NK cells (**e**) in mice in each of the three groups ( $n = 8$  mice for each group). **f** Percentages of NK cell populations in the spleen ( $n = 6$  mice for each group). CD11b-CD27- (DN), CD11b-CD27+ (CD27 SP), CD11b+CD27+ (DP), and CD11b+CD27- (CD11b SP) NK cells. **g** Strong MWA-induced cytotoxic activity of splenic NK cells ( $n = 6$  mice for each group). For all panels, data are plotted as the mean  $\pm$  SD.  $P$  values were calculated using a parametric test (\* $P < 0.05$ ; \*\* $P < 0.01$ ; \*\*\* $P < 0.001$ ; \*\*\*\* $P < 0.0001$ )

resulted in prolonged survival and inhibited the progression of lung metastasis with decreased numbers of pulmonary metastases in an EMT6 stage IV breast cancer model (Fig. S2a–c). These results suggested that MWA of primary breast cancer inhibited lung metastasis progression and improved survival.

NK cells are activated after MWA of primary breast cancer. The inhibition of lung metastases after MWA of the primary tumor may be attributable to a systemic antitumor immune response.<sup>18</sup> To determine the main type of antitumor immune response in this situation, we assessed the intratumoral infiltration of CD4+ T cells, CD8+ T cells, and NK cells in lung metastases.<sup>36,37</sup> Seven and fourteen days after treatment, pronounced recruitment of NK cells was observed in the MWA group compared with the control and surgery groups (Fig. 2a), while the accumulation of infiltrated CD4+ and CD8+ T cells in the MWA group was only slightly increased compared with that of the control and surgery groups (Fig. S3). In addition, the systemic NK-cell immune response was assessed, and the frequencies of splenic and peripheral NK cells were found to be significantly increased at 7 days after MWA and maintained up to 14 days after MWA (Fig. 2b; Fig. S4a). Notably, similar results were also obtained in the MWA group for the EMT6 model (Fig. S2d). However, such an effect was not observed in the sham surgery and sham MWA groups (Fig. S1c).

To further investigate the activity of NK cells, the expression of activating (NKp46) and inhibitory (Ly-49A) receptors was analyzed.

Higher percentages of splenic and peripheral NKp46-positive NK cells were observed, and lower percentages of Ly-49A-positive NK cells were observed at 7 and 14 days in the MWA group than in the control and surgery groups (Fig. 2d, e, Fig. S4c, d) but not in the sham surgery and sham MWA groups (Fig. S1d, e). Similar results were obtained in the EMT6 model as well (Fig. S2e, f). Next, the expression of the early activation marker CD69 was measured. Interestingly, surgery did not increase the frequency of CD69+ NK cells (Fig. 2c), which differed from the results of a previous study,<sup>34</sup> while MWA of the primary tumor increased the frequency of CD69+ NK cells compared with surgery or control treatment (Fig. 2c; Fig. S4b). Mouse NK cell maturation is a four-stage developmental program;<sup>38</sup> CD11b-CD27- (DN, immature phenotype), CD11b-CD27+ (CD27 SP, ability to secrete cytokines), CD11b+CD27+ (DP, ability to secrete cytokines), and CD11b+CD27- (CD11b SP, high cytolytic function). MWA of the primary tumor but not surgery induced the maturation of circulating and splenic NK cells (Fig. 2f; Fig. S4e).

The above results suggested that MWA of primary breast tumors stimulated NK cells. Then, NK cytotoxic function was assessed using splenic NK cells at different effector-target cell ratios (E:T ratios: 100:1, 10:1, and 1:1). The NK cells in the MWA group exhibited a higher cytotoxic capacity against target YAC-1 cells at an E:T ratio of 100:1 than those in the control and surgery groups at 7 and 14 days after MWA (Fig. 2g). To investigate the mechanisms underlying the enhanced cytotoxic function of NK



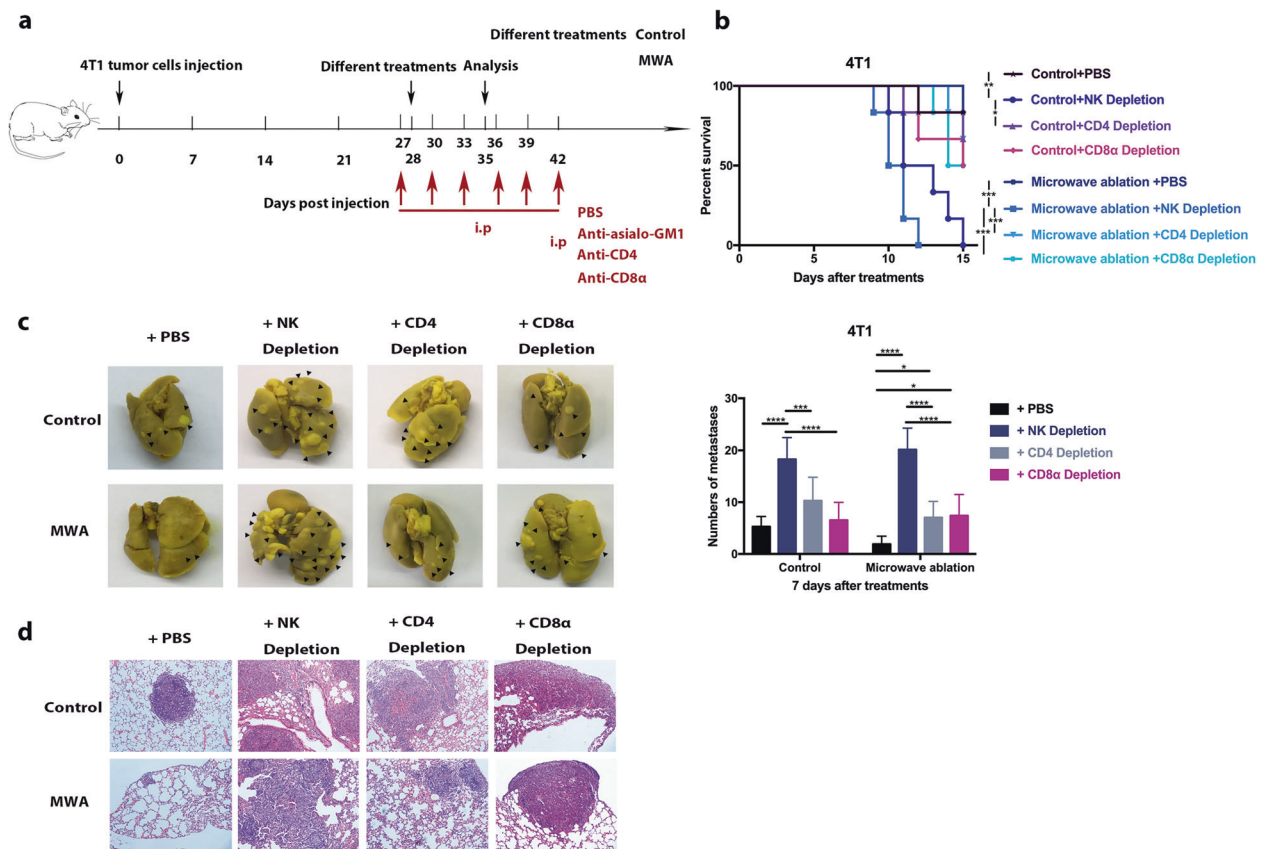


**Fig. 3** NK cells played a pivotal role in the MWA-induced regression of lung metastasis in a BALB/c mouse-derived transplantable 4T1 tumor model. **a** Schematic illustration of the experimental design for **b–d**. **b** Survival analysis of the mice in the MWA group and control group with/without CD4+ T-cell, CD8+ T-cell, or NK-cell depletion ( $n = 6$  mice for each group). Survival was analyzed using the log-rank test ( $*P < 0.05$ ;  $**P < 0.01$ ;  $***P < 0.001$ ). **c** Representative picture of lung lobes and the number of lung metastases in mice in different groups 7 days after treatment ( $n = 8$  mice for each group). **d** HE staining of lung lobes collected from mice in different groups 7 days after treatment. Scale bars, 50  $\mu\text{m}$ . For all panels, data are plotted as the mean  $\pm$  SD.  $P$  values were calculated using a parametric test ( $*P < 0.05$ ;  $**P < 0.01$ ;  $***P < 0.001$ ;  $****P < 0.0001$ )

cells, real-time polymerase chain reaction (RT-PCR) analysis of peripheral NK cells was performed, and cytotoxic pathways (mRNA expression of granzyme B, Fas ligand, TRAIL, and perforin increased significantly) were found to be activated in NK cells by MWA but not by surgery or control treatment (Fig. S4f).

#### NK cells play a pivotal role in the inhibition of metastatic progression

To determine the pivotal role of NK cells in the antitumor process, CD4+ T cells, CD8+ T cells, and NK cells were depleted separately (Fig. 3a). The depletion of NK cells in the MWA group significantly decreased survival compared with the depletion of CD4+ T cells or CD8+ T cells (Fig. 3b). The number of pulmonary metastases in NK-cell-depleted mice was greater than that in CD4+ or CD8+ T-cell-depleted mice in both the control and MWA groups (Fig. 3c). Moreover, the metastatic tumors in NK-cell-depleted mice were much larger than those in CD4+ or CD8+ T-cell-depleted mice in the MWA group (Fig. 3d), while the metastatic tumors in CD4+ or CD8+ T-cell-depleted mice were only slightly larger than those in control mice (Fig. 3d). In contrast, the metastatic tumors in the MWA group were smaller than those in control mice with depleted CD4+ or CD8+ T cells (Fig. 3d). Overall, MWA of the primary tumor in metastatic breast cancer inhibited the progression of metastasis mainly via the activation of NK cells.

#### IL-15 activates NK cells after MWA of breast cancer

The levels of NK-cell-related cytokines<sup>39</sup> in the peripheral blood were measured 7 days and 14 days after treatment. Although

similar cytokine profiles were observed in the control and surgery groups, MWA of the primary tumor induced completely different NK-cell-related cytokine profiles (Fig. 4a). The levels of the activating cytokines IL-2, IL-15, and IL-12 but not IL-18 increased significantly after MWA of the primary tumor (Fig. 4b–e). Conversely, the level of the inhibitory cytokine IL-10 decreased after MWA treatment (Fig. 4f). Furthermore, the levels of the NK-cell-produced cytokines granzyme B and TNF- $\alpha$  in the peripheral blood were increased significantly 7 days and 14 days after MWA (Fig. 4g, h), and the level of NK-cell-produced sFasL was increased only on day 7, not on day 14, after MWA (Fig. 4i). However, the levels of IFN- $\gamma$  did not change significantly in any of the three groups (Fig. 4j).

Since the above results suggested that the levels of activating cytokines, such as IL-15, were maintained at an elevated level after MWA of primary breast cancer, we hypothesized that IL-15 mainly activates NK cells after MWA of primary breast cancer. To test this hypothesis, depletion of IL-15 was performed (Fig. 5a). Seven days after IL-15 depletion, the frequencies of splenic and peripheral NK cells were decreased significantly in the MWA group (Fig. 5b; Fig. S5a). Compared with the MWA group, a lower percentage of Nkp46-positive NK cells was observed in the MWA+IL-15 depletion group (Fig. 5c; Fig. S5b), and the percentage of Ly-49A-positive NK cells was largely similar among different groups after IL-15 depletion (Fig. 5d; Fig. S5c). Consistently, more pulmonary metastases and shorter survival were observed in MWA-treated IL-15-depleted mice than in MWA only-treated mice (Fig. 5e, f).

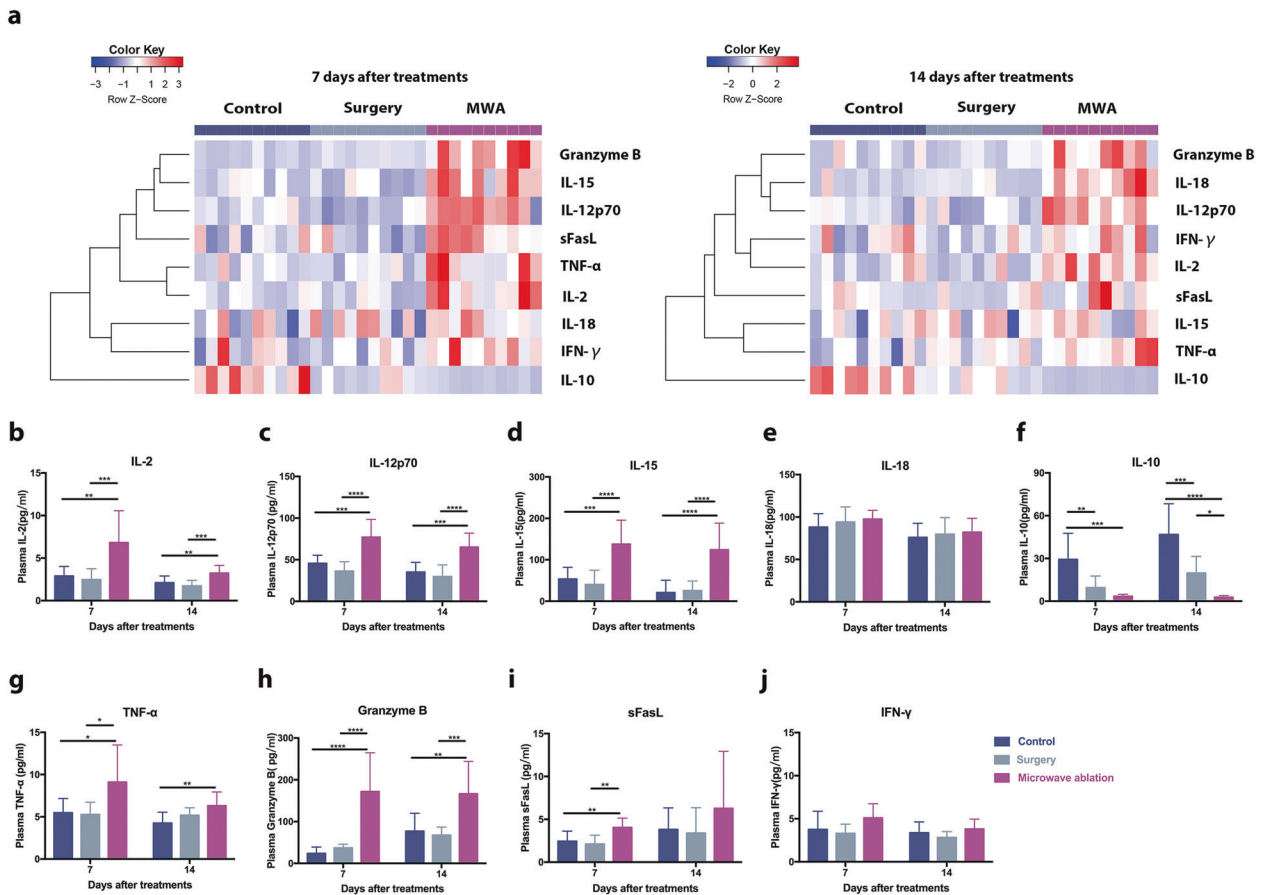


**Fig. 4** NK-cell-related cytokines were detected after microwave ablation of primary breast cancer in a BALB/c mouse-derived transplantable 4T1 tumor model. **a** Heat map of nine NK-cell-related serum cytokines 7 and 14 days after treatment in the MWA, surgery, and control groups. MWA of primary tumors induced NK-cell-related cytokine profiles completely different from those seen in the surgery and control groups ( $n = 10$  mice for each group). **b–j** Quantification of the average levels of the NK-cell-related cytokines in the three groups 7 and 14 days after treatment. For all panels, data are plotted as the mean  $\pm$  SD.  $P$  values were calculated using a parametric test (\* $P < 0.05$ ; \*\* $P < 0.01$ ; \*\*\* $P < 0.001$ ; \*\*\*\* $P < 0.0001$ )

To further validate the role of IL-15 in activating NK cells in this situation, IL-15/IL-15R $\alpha$ -Fc was given to mice in the surgery group (Fig. S6a). Compared with those in the control group and surgery group, the percentages of splenic and peripheral NK cells in the IL-15/IL-15R $\alpha$ -Fc + surgery group were significantly increased (Fig. S6b). The proportions of NKp46- and Ly-49A-positive NK cells in the peripheral blood did not increase when IL-15/IL-15R $\alpha$ -Fc was given; they only significantly increased in the spleen (Fig. S6c, d). Moreover, there were fewer pulmonary metastases in IL-15/IL-15R $\alpha$ -Fc + surgery mice than in surgery and control mice (Fig. S6e). These results suggested that IL-15 mainly activated NK cells after MWA of primary breast cancer and that surgery combined with IL-15/IL-15R $\alpha$ -Fc treatment may produce beneficial effects on stage IV breast cancer.

Macrophages are responsible for the increased IL-15 expression after MWA

The IL-15 protein is primarily produced by monocytes/macrophages and dendritic cells.<sup>40</sup> To identify the source of IL-15, RT-PCR was performed with primary tumor samples from mice in the MWA, sham MWA, and control groups (Fig. S7a, b). The mRNA levels of *CD14* (monocyte marker), *F4/80* (macrophage marker), and *CD80* (type-1 macrophage marker) in the MWA group were significantly higher than those in the control and sham MWA groups. The mRNA levels of *CD11b* in the MWA and sham MWA groups were significantly higher than those in the control group,

while the mRNA level of *CD206* (type-2 macrophage marker) was significantly lower in the MWA group than in the other two groups. Intriguingly, the mRNA levels of *CD11c* (dendritic cell marker) and *LY6G* (neutrophil marker) in the three groups were similar. Immunohistochemical staining showed that the level of F4/80 in the MWA group was higher than that in the other two groups (Fig. S7c). Collectively, these results suggested that the accumulated macrophages were activated in the primary tumor after MWA. Moreover, the mRNA levels of *IL-15* and *CD49b* in the MWA group were significantly higher than those in the control and sham MWA groups (Fig. S7b).

We therefore reasoned that IL-15 was mainly produced by infiltrated macrophages after MWA in this study. To test this hypothesis, clophosome-A (negatively charged clodronate liposomes) was injected into the primary tumor after MWA to deplete macrophages (Fig. 6a). Serum IL-15 levels were significantly decreased in the macrophage depletion group compared with the MWA only group 7 days after MWA (Fig. 6b). Subsequently, the percentages of peripheral and splenic NK cells were significantly decreased in the MWA group (Fig. 6c; Fig. S8a). The percentage of splenic NKp46-positive NK cells was also decreased in the MWA + macrophage depletion group compared with the MWA group (Fig. 6d), while the percentages of peripheral and splenic Ly-49A-positive NK cells were similar between the MWA + macrophage depletion and MWA only groups (Fig. 6e; Fig. S8b, c). Moreover, a larger number of pulmonary metastases and shorter survival were

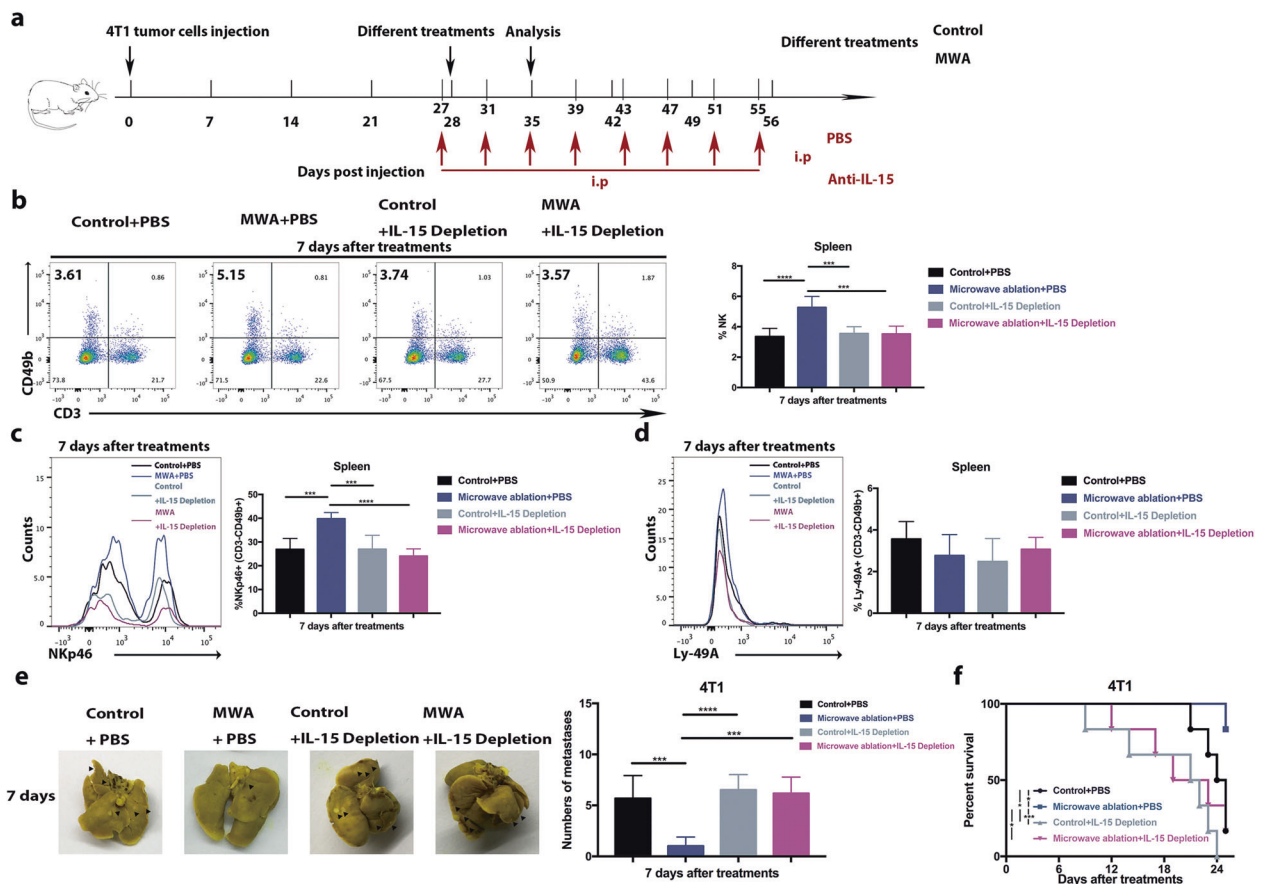


**Fig. 5** The MWA-induced NK-cell response was mainly activated by IL-15 in the BALB/c mouse-derived transplantable 4T1 tumor model. **a** Schematic illustration of the experimental design for **b–f** ( $n = 6$  mice for each group). The percentages of splenic NK cells (**b**), NKp46-positive NK cells (**c**), and Ly-49A-positive NK cells (**d**) 7 days after IL-15 depletion. **e** Representative picture of lung lobes and the number of lung metastases in mice from different groups. For the above panels, data are plotted as the mean  $\pm$  SD.  $P$  values were calculated using a parametric test (\* $P < 0.05$ ; \*\* $P < 0.01$ ; \*\*\* $P < 0.001$ ; \*\*\*\* $P < 0.0001$ ). **f** Survival analysis of the mice in the MWA group and control group with IL-15 depletion using the log-rank test (\* $P < 0.05$ ; \*\* $P < 0.01$ ; \*\*\* $P < 0.001$ )

observed in the MWA+ macrophage depletion group than in the MWA only group (Fig. 6f, g). These findings suggested that the macrophages infiltrated and were activated after MWA of the primary tumor; these cells then produced IL-15 that activated NK cells to inhibit the progression of metastasis in stage IV breast cancer (Fig. 7).

MWA of human breast cancer stimulates the NK-cell response  
MWA has been applied to treat some types of small breast cancer in our center. In the present study, 14 patients were recruited between July 2016 and December 2018, and their peripheral blood was examined before and 1 week after MWA (Fig. 8a). Another 14 early-stage breast cancer patients who received standard surgery were selected as the control group (Fig. 8a). The baseline characteristics of these patients are summarized in Supplementary Table 1. Among the peripheral lymphocytes analyzed, the percentage of CD3–CD56+ NK cells was significantly increased at 1 week after MWA compared with before MWA (18.83  $\pm$  5.40% basal, 24.56  $\pm$  9.45% week 1,  $P < 0.05$ ,  $n = 14$ , Fig. 8b). However, the percentage of CD3–CD56+ NK cells was not significantly different before and after surgery ( $n = 14$ , Fig. 8b). Moreover, the increase in the CD3–CD56+ NK-cell percentage in the MWA group was significantly higher than that in the surgery group (Fig. 8b).

To characterize the effect of MWA on NK cells, the percentage of CD16+CD3–CD56+ cytotoxic NK cells was analyzed (Fig. 8c). Among CD3–CD56+ NK cells, the proportion of CD16+

CD3–CD56+ cells was increased significantly 1 week after MWA (92.46  $\pm$  5.44% basal, 94.45  $\pm$  3.53% week 1,  $n = 14$ ,  $P < 0.05$ ), but no significant change was observed in the surgery group ( $n = 14$ , Fig. 8c). The increase in the CD16+ NK-cell percentage in the MWA group was significantly higher than that in the surgery group (Fig. 8c). To further investigate the activation status of NK cells, the expression of activating and inhibitory receptors was analyzed. The NKp46+CD3–CD56+ cell percentage was increased significantly 1 week after MWA ( $n = 12$ , Fig. 8d) but not after surgery ( $n = 11$ , Fig. 8d). The percentage of NK cells expressing the inhibitory receptor NKG2A increased significantly in the surgery ( $n = 14$ ) group but not in the MWA group ( $n = 14$ , Fig. 8e).

Furthermore, to confirm the role of IL-15 in the activation and secretory function of NK cells, the concentrations of serum IL-15 (Fig. 8f), granzyme B (Fig. 8g), and FasL (Fig. 8h) were measured in the surgery ( $n = 8$ ) and MWA groups ( $n = 10$ ). The levels of serum IL-15, granzyme B, and FasL increased significantly in the MWA group but not in the surgery group. Strikingly, the increases in the IL-15 and granzyme B levels, but not the FasL level, were significantly higher in the MWA group than in the surgery group.

Finally, the potential effect of surgical injury on the NK-cell response was excluded by determining the differences between lumpectomy and mastectomy in the surgery group. Similar trends were observed in patients undergoing either lumpectomy or mastectomy (Fig. 8b–h). Taken together, these results coherently suggested that MWA of human breast cancer stimulated an autologous NK-cell response.



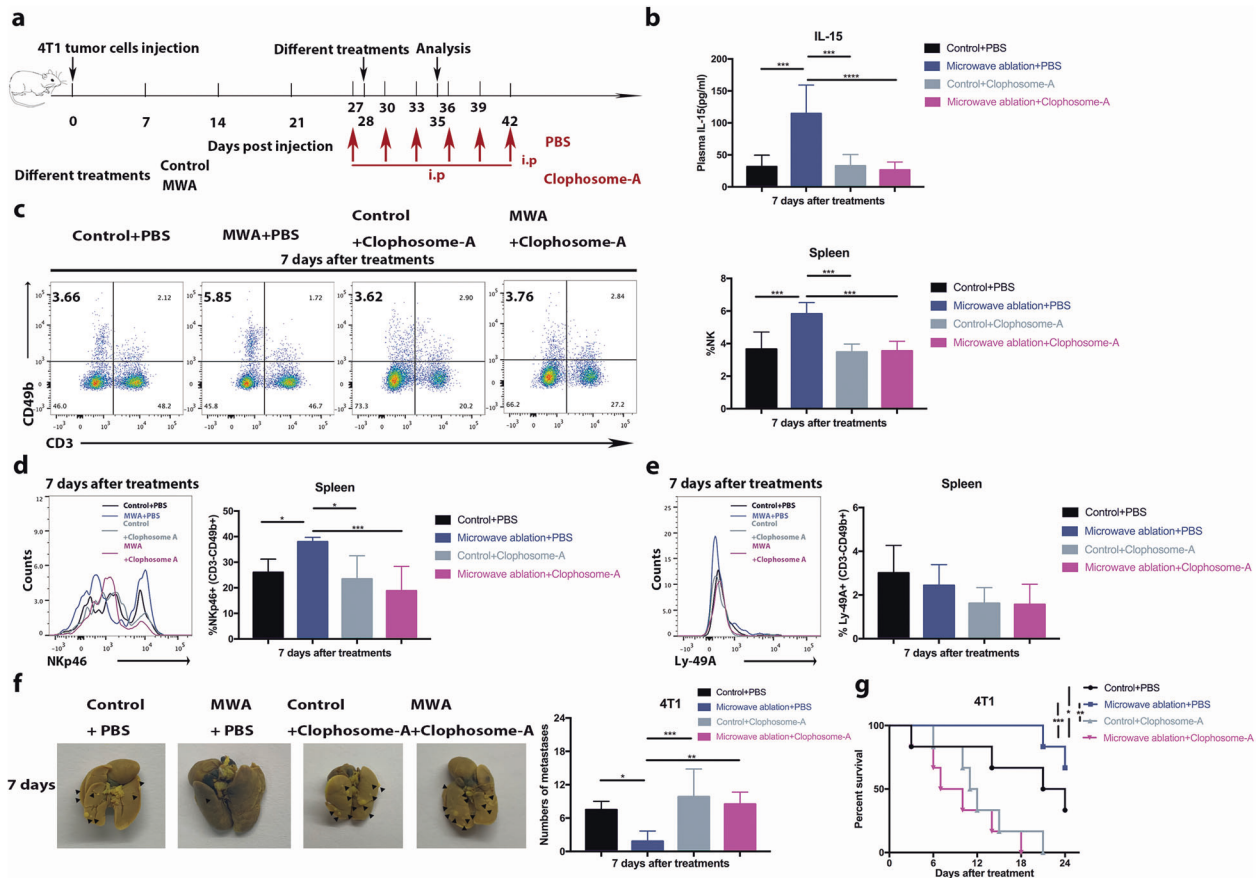


**Fig. 6** Macrophages were responsible for the MWA-induced NK-cell response in the BALB/c mouse-derived transplantable 4T1 tumor model. **a** Schematic illustration of the experimental design for **b–g** ( $n = 6$  mice for each group). **b** Serum IL-15 levels 7 days after treatment with/without macrophage depletion. The percentages of splenic NK cells (**c**), NKp46-positive NK cells (**d**), and Ly-49A-positive NK cells (**e**) 7 days after treatment with macrophage depletion. **f** Representative picture and the numbers of metastases in lung lobes from different groups. For the above panels, data are plotted as the mean  $\pm$  SD.  $P$  values were calculated using a parametric test (\* $P < 0.05$ ; \*\* $P < 0.01$ ; \*\*\* $P < 0.001$ ; \*\*\*\* $P < 0.0001$ ). **g** Survival analysis of the mice in the MWA group and control group with macrophage depletion using the log-rank test (\* $P < 0.05$ ; \*\* $P < 0.01$ ; \*\*\* $P < 0.001$ )

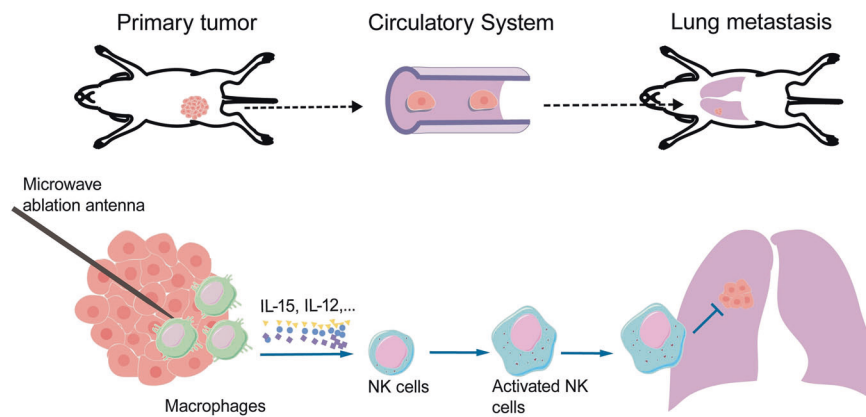


**Fig. 7** Microwave ablation of primary breast cancer inhibits metastatic tumor progression via the macrophage/IL-15/NK-cell axis

**DISCUSSION**

Stage IV breast cancer is an incurable disease, and locoregional treatment of primary tumors often results in distant progression. However, surgery is essential for controlling symptoms and complications in a subset of patients. Therefore, the local control of de novo stage IV breast cancer seems to be an intractable problem. The current study offers a promising treatment strategy for patients with de novo stage IV breast cancer. MWA not only controlled the primary tumor but also inhibited the progression of

metastasis. This abscopal effect could be attributed to the activation of NK cells after MWA of the primary tumor in two stage IV breast cancer models. In addition, a strong NK-cell response was observed after MWA of breast cancer in clinical practice. Collectively, these results indicated that the systemic NK-cell response following MWA of breast cancer might induce regression of distant metastases.

Previous studies<sup>41,42</sup> suggest that the bone, lungs, liver, and brain are the niches suitable for metastasis in breast cancer

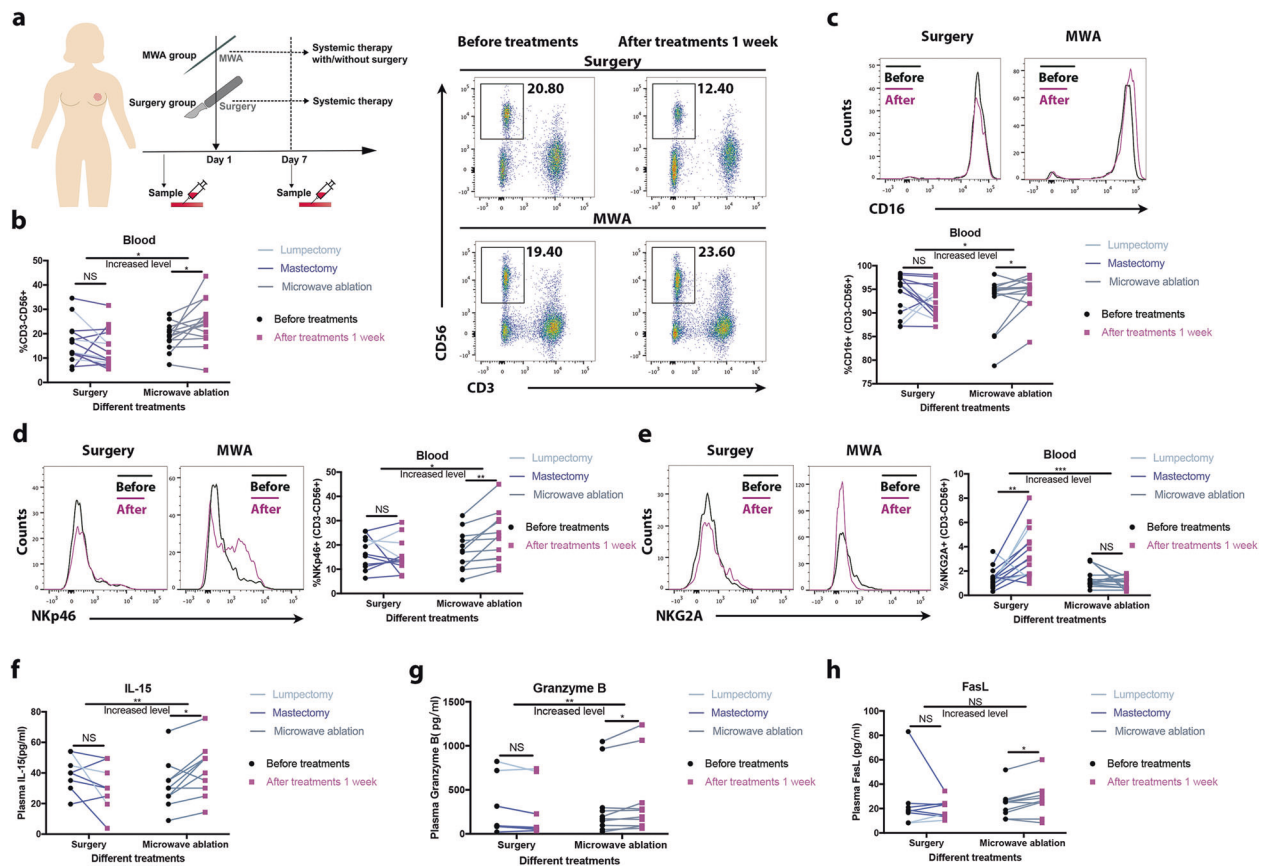


**Fig. 8** NK cells were activated after MWA of early-stage breast cancer in the clinic. **a** Schematic illustrating the experimental design for **b–h**. The percentages of peripheral NK cells (**b**), CD16<sup>+</sup> NK cells (**c**), NKp46<sup>+</sup> NK cells (**d**), and NKG2A<sup>+</sup> NK cells (**e**) before and 7 days after treatment in the surgery group and MWA group. Serum IL-15 (**f**), granzyme B (**g**), and FasL levels (**h**) before and 7 days after treatment in the surgery group and MWA group. For all panels, data are plotted as the mean ± SD. *P* values were calculated using the parametric test (\**P* < 0.05; \*\**P* < 0.01; \*\*\**P* < 0.001; \*\*\*\**P* < 0.0001)

patients and that distant metastatic sites exert a significant prognostic impact on survival. Patients with visceral metastases have poorer survival than patients with nonvisceral metastases.<sup>43</sup> Although lung metastases are less life restricting than liver and brain metastases, many patients still die from lung metastasis, which is the most common type of visceral metastasis.<sup>41,42</sup> In this study, 4T1 and EMT6 tumor models were applied, which are ideal pulmonary metastasis models.<sup>34,44</sup> We found that MWA of the primary tumor inhibited the progression of lung metastases. However, the effects of this immune response on metastases in other sites should be determined in the future.

The antitumor immunity induced by MWA has been reported in only a few studies,<sup>18,31,32,45,46</sup> and MWA is a weak stimulator of the adaptive immune response. Other studies suggest that cryoablation induces notably higher postablative immunogenicity than radiofrequency ablation or MWA<sup>18,47</sup> and that cryoablation is associated with high levels of IL-1, IL-6, and TNF-α.<sup>45,48</sup> However, the innate immune response induced by thermal therapies has seldom been reported.<sup>15</sup> The present study demonstrated that a robust NK-cell response was induced by MWA of breast cancer but not by primary tumor resection. Previous studies suggest that tumor resection may partially reverse tumor-induced T-cell immunosuppression.<sup>34,49</sup> However, no significant T-cell immune response was observed after surgery in this study. Thus, tumor burden reduction alone might not activate NK cells and T cells. In addition, only a weak T-cell response was observed after MWA in this and previous studies.<sup>31,32</sup> Overall, a strong NK-cell response after MWA inhibits the progression of metastasis in stage IV breast

cancer, although the differences in postablative immunogenicity induced by different ablation methods should still be determined in the future.

IL-12, IL-18, IL-15, type I interferon, and IL-2 are reported to be potent activators of NK cells.<sup>50</sup> Herein, we observed that IL-15 effectively activated NK cells after MWA of breast cancer, while IL-2 and IL-12 only partially activated NK cells. Interestingly, we found that NK cells could be activated in the surgery group when IL-15/IL-15Rα-Fc was administered, suggesting that surgery plus IL-15/IL-15Rα-Fc treatment may also be potentially effective in treating stage IV breast cancer.

Macrophages and DCs, stimulated by the release of intracellular contents after ablation,<sup>18,51,52</sup> constitute a source of cytokines to trigger NK-cell activation.<sup>53</sup> Intratumoral macrophages and dendritic cells are associated with released IL-15 and IL-12 after MWA.<sup>54</sup> In addition, we found that the level of IL-15 and the percentage of peripheral NK cells were significantly decreased after intratumoral depletion of macrophages post MWA. These results suggested that macrophages were activated in primary tumors after MWA and released most of the transpresented IL-15 to stimulate NK cells, which has been documented previously.<sup>55</sup> Thus, decreased mouse survival was associated with blockade of the interaction between macrophages and NK cells<sup>56</sup> when intratumoral macrophages were depleted after MWA.

In addition, a weak T-cell response was observed after MWA of breast cancer, which might be associated with the increased IL-12 and IL-2 levels. Importantly, IL-12 induces T cells to differentiate into Th1 cells and stimulates IFN-γ production by Th1 cells.<sup>57</sup> IL-2 is



crucial in the expansion of CD8<sup>+</sup> T cells and the functional maturation of activated T cells.<sup>58</sup> In the present study, depletion of CD4<sup>+</sup> or CD8<sup>+</sup> T cells did not significantly decrease the survival of mice after MWA of the primary tumor; however, the number of pulmonary metastases increased significantly. In the short-term after MWA, the T-cell response was weak. However, the long-term effect of T cells should be determined in the future.

Although there is a growing trend toward applying minimally invasive thermal therapies, surgery is still the standard therapy for breast cancer.<sup>23,30</sup> Considering the advantages of thermal therapy over surgery, the clinical outcomes of small breast cancer patients treated with MWA were assessed in our center. Importantly, the immune response was evaluated before any systemic therapy was administered. To avoid the bias caused by systemic therapy, we did not assess the NK-cell response in stage IV breast cancer, although the basic immune statuses are different between early and advanced breast cancer. Clinically, peripheral NK cells were activated 7 days after MWA of early breast cancer tumors; however, the clinical effect of this innate immune response was not clarified in de novo stage IV breast cancer. Although subgroup analysis could not be performed at the current stage, both hormone receptor-positive and hormone receptor-negative breast cancer may exhibit an NK-cell response following MWA based on our experimental and clinical data. Moreover, whether the NK-cell response is thermal dose dependent is not clear because of the sample size and limited thermal dose discrepancies. Due to the large variation in clinical data and small sample size, the systemic effects of the MWA-induced NK-cell response on breast cancer remain to be explored clinically.

Furthermore, minimally invasive thermal therapies are promising approaches for the treatment of breast cancer,<sup>23–27</sup> with high rates of complete ablation observed, particularly for MWA. Therefore, MWA may be effective for the local control of symptoms and complications in stage IV breast cancer. Importantly, the immunomodulatory processes activated by thermal therapies are under intensive investigation.<sup>18</sup> The current study provides strong evidence for the systemic NK-cell response in breast cancer to MWA.

## MATERIALS AND METHODS

### Study design

The present study aimed to determine the immunomodulatory effect of MWA treatment of primary breast cancer on lung metastasis in murine models of stage IV breast cancer. A minimum of six mice per group per experiment were used, and consistent results were obtained. The animals were age- and size-matched across all groups. All animal procedures were approved by the institution Animal Care and Use Committee, Nanjing Medical University.

MWA was approved for the treatment of solid tumors by the China Food and Drug Administration and is applied for the treatment of small breast cancer in our center with cautious indications. Patients underwent only MWA without standard surgery if they declined or were unsuitable for surgery due to medical conditions, and long-term outcomes were assessed. Other patients underwent standard surgery ~1 week after MWA according to the guidelines of our center, and short-term outcomes were assessed by pathology. After MWA or surgery, other systemic treatments were recommended according to the guidelines. Peripheral blood was obtained from patients and analyzed at the indicated time points to confirm the NK-cell response induced by MWA.

### Patient enrollment and treatments

Patients diagnosed with invasive breast cancer were recruited for MWA in the current prospective nonrandomized study. The eligibility criteria included the following: (a) a single tumor with

a maximal diameter ≤ 3 cm proven by ultrasound and mammography; (b) invasive breast cancer proven using core-needle biopsy with a sufficient sample for the analysis of hormone receptor, human epidermal growth factor receptor 2, and Ki67 statuses; and (c) both the skin and pectoralis major muscle not infiltrated by the tumor. The exclusion criteria included the following: (a) patients with an extensive intraductal component in the invasive cancer; (b) patients who were pregnant or breastfeeding; and (c) tumor located in the nipple-areola area.

Ultrasound was used to guide MWA and monitor the procedure. Local lidocaine anesthesia was administered, and the antenna was placed into the tumor along the largest axis. Before MWA, hydrodissection was performed. The microwave irradiation frequency of the system (Nanjing Yigao Microwave Electric Institute, Nanjing, China) was 2450 MHz with the output power set at 40 W. During the MWA procedure, there was a gradual diffuse increase in the echogenicity of the tumor from the irradiating segment to the whole tumor. According to previous data and the tumor sizes included in this study, MWA with an output power of 40 W for at least 2 min was recommended to achieve complete ablation, which was defined as the tumor disappearing completely on ultrasound.

### Cell lines and culture

The murine mammary carcinoma cell lines 4T1 and EMT6 and the murine lymphoma cell line YAC-1 were purchased from the Chinese Academy of Sciences (Shanghai, China). The cells were cultured in RPMI-1640 medium (HyClone, USA) supplemented with 10% fetal bovine serum, 100 µg/mL streptomycin, and 100 units/mL penicillin (Shanghai Sangon, China) at 37 °C with 5% CO<sub>2</sub>.

### Mice and tumor models

Six-to-eight-week-old female Balb/c mice were purchased from the Animal Model Research Center of Nanjing University and maintained under specific pathogen-free conditions in the Animal Core Facility of Nanjing Medical University. In total, 1 × 10<sup>5</sup> 4T1 or EMT6 cells in 100 µL of PBS were injected subcutaneously into the right inguinal mammary fat pads of each animal.

### Mouse treatment procedures

Subcutaneous injection of murine 4T1 or EMT6 cells into Balb/c mice led to the formation of primary tumors and spontaneous metastasis to the lungs. At 28 days after 4T1 cell injection or 16 days after EMT6 cell injection, when the tumor diameter was >8 mm (range, 8–10 mm), the mice were divided into three groups: untreated tumors (control), MWA-treated tumors (MWA), and surgically treated tumors (surgery). The mice were anesthetized using inhaled isoflurane (RWD Life Science, Shenzhen, China). The tumor site was sanitized with a 75% ethanol tincture before treatment. All the procedures were performed aseptically. For MWA, an output power of 5 W was applied using a microwave generator (ECO-100E, Yigao Microwave Electric Institute, Nanjing, China) with an irradiation frequency of 2450 MHz. According to preliminary data, MWA with an output power of 5 W for 3 min can completely ablate tumors with a diameter of ~8–10 mm in mice. Therefore, MWA with an output power of 5 W was performed on every tumor in mice for 3 min in this study. For surgery, a 1.5-cm incision was made around the tumor to guarantee complete resection of the tumor. Finally, the wound was sutured with 4/0 nylon.

### Lung metastasis analysis

4T1 or EMT6 cells (1 × 10<sup>5</sup>) were injected as described above. Mice were sacrificed on day 7 or 14 after treatment, and the lungs were either harvested in Bouin's solution (75 mL of saturated picric acid, 25 mL of 4% paraformaldehyde, and 5 mL of glacial acetic acid) to count the number of surface tumors or fixed in 4% formalin, embedded in paraffin, sectioned and stained with hematoxylin-eosin.

### Immunohistochemical analysis

Paraffin sections of mouse lungs were stained with an anti-mouse cleaved caspase 3 antibody (Asp175, CST), anti-mouse VEGF antibody (JH121, Thermo Fisher Scientific), anti-mouse CD4 antibody (4SM95, eBioscience), anti-mouse CD8 antibody (4SM15, eBioscience), anti-mouse CD49b antibody (HMa2, eBioscience), and anti-mouse F4/80 antibody (BM8, eBioscience). Next, the samples were incubated with horseradish peroxidase (HRP)-conjugated goat anti-rat IgG (Santa Cruz Biotechnology, Santa Cruz, CA, USA), followed by incubation with 3,3'-diaminobenzidine (DAB Kit, Beyotime, Nanjing, China) to visualize the immunocomplexes.

### Mouse single-cell suspensions

At least six mice were euthanized, and blood was collected retro-orbitally into EDTA-K2 tubes. In addition, spleens and lungs were harvested. The blood was treated with RBC lysis buffer (eBioscience) to remove the red blood cells and obtain a single-cell suspension. The harvested spleen was crushed gently with the plunger of a 10-mL syringe and passed through a 40- $\mu$ m nylon mesh cell strainer (Falcon, New Jersey, USA) to obtain a single-cell suspension. Subsequently, all single-cell suspensions were resuspended in flow cytometry staining buffer.

### Isolation of peripheral blood mononuclear cells (PBMCs)

Peripheral blood (6 mL) was collected from patients on the day before surgery and 1 week after MWA or surgery into EDTA-K2 tubes. Then, the PBMCs were isolated from the fresh anticoagulant-treated blood by Ficoll discontinuous density gradient centrifugation and resuspended in flow cytometry staining buffer for flow cytometric analysis.

### Flow cytometry

Cells were stained for surface markers in flow cytometry staining buffer at 4 °C for 30 min after Fc blocking to characterize murine immune cell subsets. The following antibodies were used: FITC-conjugated anti-mouse CD3 (clone 145-2C11, BioLegend), PE-conjugated anti-mouse CD49b (clone DX5, BioLegend), PE/Cy7-conjugated anti-mouse CD49b (clone DX5, BioLegend), PerCP-Cy5.5-conjugated anti-mouse CD69 (clone H1.2F3, BioLegend), PE-conjugated anti-mouse CD335 (NKp46) (clone 29A1.4, eBioscience), Pacific Blue™-conjugated anti-mouse Ly-49A (clone YE1/48.10.6, BioLegend), APC-conjugated anti-mouse/rat/human CD27 (clone LG.3A10, BioLegend), and PE/Cy7-conjugated anti-mouse CD11b (clone M1/70, eBioscience). Fresh PBMCs obtained from patients were stained with FITC-conjugated anti-human CD3 (clone OKT3, BioLegend), PE/Cy7-conjugated anti-human CD56 (clone 5.1H11, BioLegend), Brilliant Violet 421™-conjugated anti-human CD16 (clone 3G8, BioLegend), PE-conjugated anti-hNKG2A (clone 131411, R&D Systems), and APC-conjugated anti-human CD335 (NKp46) (clone 9-E2, BD) antibodies. Flow cytometric analysis was performed using a BD FACSAria II cytometer (BD Biosciences), and data were analyzed using FlowJo software.

### Purification of mouse NK cells

NK cells from the spleen or peripheral blood were sorted on a FACSAria cell sorter (BD Bioscience), and the purity of the NK cells was  $\geq 95\%$ . The isolated NK cells were processed for cytotoxicity assays or used for RNA extraction. The cells were cultured in RPMI-1640 medium supplemented with 10% FBS, 1% streptomycin, and 1% penicillin.

### Cytotoxicity assay with NK cells and YAC-1 cells

Splenic NK cells (Effector-E) were sorted on a FACSAria cell sorter (BD Bioscience). YAC-1 cells (Target-T) were cultured in RPMI-1640 medium supplemented with 10% FBS, 1% streptomycin, and 1% penicillin at 37 °C in 5% CO<sub>2</sub>. The purity of the NK cells was  $\geq 95\%$ , and the activity of the YAC-1 cells was  $\geq 98.5\%$ . The splenic NK and

YAC-1 cells were seeded in six-well plates at an E:T ratio of 1:1, 10:1, or 100:1 and incubated with 100 U/m rhIL-2 (PeproTech) for 24 h, followed by centrifugation at 450  $\times g$  for 6 min. The cell mixtures were stained with 7-AAD, and then staining for a surface marker on mouse NK cells with a PE-conjugated anti-mouse CD49b antibody (clone DX5, BioLegend) was performed in flow cytometry staining buffer at 4 °C for 30 min, followed by Fc blocking to characterize the splenic NK cells and distinguish the YAC-1 cells. The percentage of cytotoxicity was calculated according to the formula: 100  $\times$  apoptotic YAC-1 cells/total YAC-1 cells.

### Cytokine analysis

Peripheral blood was collected from the intraocular canthal vein of mice on day 7 or 14 after different treatments, and the serum layer was isolated by centrifugation at 10,000  $\times g$  for 10 min. Murine plasma was analyzed to detect the concentrations of IL-2, IL-12p70, IL-15, IL-18, IL-10, IFN- $\gamma$ , TNF, sFasL, and granzyme B using the MILLIPLEx<sup>MAP</sup> Mouse Cytokine/Chemokine Magnetic Bead Panel (Millipore, Macquarie Park, NSW, Australia), MILLIPLEx<sup>MAP</sup> Mouse CD8+ T Cell Magnetic Bead Panel (Millipore), IL-18 Platinum ELISA Kit (eBioscience), and Mouse IL-15/IL-15R ELISA Kit (MultiSciences) according to the manufacturer's instructions.

Peripheral blood (6 mL) was collected from patients into EDTA-K2 tubes on the day before treatment and 1 week after treatment. The plasma fraction was isolated from the whole blood by centrifugation at 10,000  $\times g$  for 10 min. The concentrations of IL-15, sFasL, granzyme B, and perforin in the plasma were measured using the appropriate human ELISA kit. The serum was stored at -80 °C until further analysis.

### In vivo immune cell depletion

For NK-cell depletion, 25  $\mu$ L of anti-asialo GM1 antibody (986-10001; Wako Pure Chemical Industries Ltd) was diluted in 75  $\mu$ L of PBS and injected intraperitoneally into mice. T cells were depleted by intraperitoneal injections of anti-mouse CD8 $\alpha$  (clone 53.6.72; 200  $\mu$ g per mouse; BioXCell) or anti-mouse CD4 antibodies (clone GK1.5, 200  $\mu$ g per mouse; BioXCell). All injections were started 1 day before treatment initiation and continued during the experiment. Macrophages were depleted by intraperitoneal injection of 200  $\mu$ L of Clophosome®-A-anionic clodronate liposomes (Clophosome-A; F70101C-A; FormuMax Scientific) into each mouse one day prior to treatment initiation, followed by injection of 100  $\mu$ L every 3 days. Control mice were treated with PBS.

### Treatment with an anti-IL-15 antibody

For cytokine neutralization, a neutralizing mouse anti-IL-15 antibody was purchased from R&D Systems. An equivalent of 15  $\mu$ g/mL mouse anti-IL-15 antibody (catalog AF447; R&D Systems) was injected intraperitoneally in a volume of 100  $\mu$ L one day prior to therapy and at 4-day intervals. Control mice were treated at the same time with PBS.

### IL-15/IL-15Ra-Fc complex treatment

IL-15/IL-15Ra-Fc complexes were generated by mixing and incubating recombinant murine IL-15 (PeproTech) and recombinant mouse IL-15Ra-Fc (R&D Systems) together in PBS at 37 °C for 30 min at a ratio of 1:6. In this study, IL-15/IL-15Ra-Fc complexes (0.5  $\mu$ g of IL-15 and 3  $\mu$ g of IL-15Ra-Fc in 200  $\mu$ L of PBS per mouse) were intraperitoneally injected into mice beginning on the day before treatment and then administered every other day. Control mice were treated at the same time with PBS.

### RNA isolation and real-time quantitative PCR

Total RNA was extracted from purified NK cells or primary tumor tissue using an RNeasy Mini kit (Qiagen, Germany) according to the manufacturer's instructions. Absorbance was measured at 260/280 nm to assess the purity of the isolated mRNA (high purity

defined as a ratio > 1.86). cDNA was synthesized using PrimeScript RT Master Mix (TaKaRa). Specific primers from Invitrogen (Shanghai, China) were used for quantitation of transcript levels. All quantitative real-time PCR assays were performed using SYBR Premix Ex Taq II (TaKaRa) on a StepOne Plus Real-Time PCR system (Applied Biosystems, USA) in 96-well plates. Data were analyzed by the  $2^{-\Delta\Delta CT}$  method. The primer sequences for mouse genes were as follows: *GAPDH*: forward 5'-GGTGAAGGTCGGTGTGAA CG-3', reverse 5'-CTCGCTCCTGGAGATGGTG-3'; *granzyme B*: forward 5'-TCTCGACCTACATGGCCTTA-3', reverse 5'-TCCTGTCTT TGATGTTGTGGG -3'; *FasL*: forward 5'-TCCGTGAGTTCACCAACC AAA-3', reverse 5'-GGGGTTCCTGTAAATGGG-3'; *Perforin*: forward 5'-CTGCCACTCGGTGAGAATG-3', reverse 5'-CGGAGGGTAGTC ACATCCAT-3'; *TRAIL*: forward 5'-ATGGTGATTGCATAG-3', reverse 5'-GCAAGCAGGGTCTGT-3'; *NKp46*: forward 5'-ATGCTGCCAACACT ACTG-3', reverse 5'-GATGTTACCGAGTTTCCATTG-3'; *CD49b*: forward 5'-TGCTGGCGTATAATGTTGGC-3', reverse 5'-CTTGTGGGT TCCTAAGCTGCT-3'; *F4/80*: forward 5'-TGACTACCTGTGCTCCT AA-3', reverse 5'-CTTCCAGAAATCCAGTCTTTCC-3'; *CD80*: forward 5'-GCAGGATACACCCTCTCAA-3', reverse 5'-AAAGCAAGTACAGC AGCACAA-3'; *CD206*: forward 5'-CTCTGTTGCTATTGGACGC-3', reverse 5'-CGGAATTTCTGGGATTGAGTTC-3'; *CD11b*: forward 5'-CCATGACCTTCCAAGAGAATGC-3', reverse 5'-ACCGCTTGTGCTGT AGTC-3'; *CD11c*: forward 5'-CCAAGACATCGTGTCTCTGATT-3', reverse 5'-ACAGCTTAAACAAAGTCCAGCA-3'; *LY6C*: forward 5'-GC AGTGCTACGAGTGTATGG-3', reverse 5'-ACTGACGGGTCTTTAGTT TCCTT-3'; *LY6G*: forward 5'-GACTTCCTGCAACACAACACTACC-3', reverse 5'-ACAGCATTACCAGTGTCTCAGT-3'; *CD14*: forward 5'-CTCTGCTTAAAGCGGCTTAC-3', reverse 5'-GTTGCGGAGGTTCAAG ATGTT-3'; *CD68*: forward 5'-TGCTGATCTGCTAGGACCG-3', reverse 5'-GAGAGTAACGGCCTTTTGTGA-3'; and *IL-15*: forward 5'-CATCCATCTGCTACTTGTG-3', reverse 5'-GCCTGCTTTTAGGG AGACCT-3'. All the experiments were performed in triplicate, and the expression of the target genes was calculated and normalized to that of the endogenous control *GAPDH* gene.

#### Statistics

Numerical data are reported as the mean  $\pm$  standard deviation (SD). The significance of differences among groups was assessed by a parametric test (GraphPad Prism v5.0). The survival rate was analyzed with the Kaplan–Meier method using the log-rank test. In the clinic, the difference in parameters before and after MWA or surgery was assessed by a paired Student's *t* test. A *P* value < 0.05 was considered statistically significant. \**P* < 0.05; \*\**P* < 0.01; \*\*\**P* < 0.001; \*\*\*\**P* < 0.0001.

#### Declarations

The study was reviewed and approved by the institutional ethics committee of The First Affiliated Hospital of Nanjing Medical University (2010-SR-003) and was retrospectively registered on June 19, 2019, in the Chinese Clinical Trial Registry (registration number ChiCTR1900023959). Informed consent was obtained from all patients. All experimental methods were in accord with the Helsinki Declaration.

#### ACKNOWLEDGEMENTS

This work was supported in part by the National Natural Science Foundation of China (81771953), the Six Kinds of Outstanding Talent Foundation of Jiangsu Province (WSW-014, to W.Z.), the Natural Science Foundation of Jiangsu Province (BK20180108), and a project funded by the Priority Academic Program Development of Jiangsu Higher Education Institutions (PAPD).

#### AUTHOR CONTRIBUTIONS

W.Z. and S.W. contributed to the conception and design of the study, the analysis and interpretation of data and the revision of the article, and provided final approval of the version to be submitted. M.Y., H.P., L.L., C.W., Y.W., G.M., M.Q., and J.L. performed

the experimental study and statistical analysis and drafted and revised the article. N.C., M.Z., H.X., L.L., X.G., and Y.Z. participated in the clinical study, performed the statistical analysis, and drafted and revised the article. All authors read and approved the final version of the manuscript. M.Y., H.P., and L.L. contributed equally to this work. We would like to thank all the members of the SW and NC laboratories for helpful discussions and comments.

#### ADDITIONAL INFORMATION

The online version of this article (<https://doi.org/10.1038/s41423-020-0449-0>) contains supplementary material.

**Competing interests:** The authors declare no competing interests.

#### REFERENCES

- Harris, E., Barry, M. & Kell, M. R. Meta-analysis to determine if surgical resection of the primary tumour in the setting of stage IV breast cancer impacts on survival. *Ann. Surg. Oncol.* **20**, 2828–2834 (2013).
- Bafford, A. C. et al. Breast surgery in stage IV breast cancer: impact of staging and patient selection on overall survival. *Breast Cancer Res Treat.* **115**, 7–12 (2009).
- Soran A. et al. Randomized trial comparing resection of primary tumor with no surgery in stage IV breast cancer at presentation: protocol MF07-01. *Ann Surg Oncol.* **25**, 3141–3149 (2018).
- Badwe, R. et al. Locoregional treatment versus no treatment of the primary tumour in metastatic breast cancer: an open-label randomised controlled trial. *Lancet Oncol.* **16**, 1380–1388 (2015).
- Gunduz, N., Fisher, B. & Saffer, E. A. Effect of surgical removal on the growth and kinetics of residual tumor. *Cancer Res.* **39**, 3861–3865 (1979).
- Fisher, B., Gunduz, N., Coyle, J., Rudock, C. & Saffer, E. Presence of a growth-stimulating factor in serum following primary tumor removal in mice. *Cancer Res.* **49**, 1996–2001 (1989).
- Demicheli, R., Retsky, M. W., Swartzendruber, D. E. & Bonadonna, G. Proposal for a new model of breast cancer metastatic development. *Ann. Oncol.* **8**, 1075–1080 (1997).
- Al-Sahaf, O., Wang, J. H., Browne, T. J., Cotter, T. G. & Redmond, H. P. Surgical injury enhances the expression of genes that mediate breast cancer metastasis to the lung. *Ann. Surg.* **252**, 1037–1043 (2010).
- Krall J. A. et al. The systemic response to surgery triggers the outgrowth of distant immune-controlled tumors in mouse models of dormancy. *Sci Transl Med.* **10**, eaan3464 (2018).
- Coffey, J. C. et al. Excisional surgery for cancer cure: therapy at a cost. *Lancet Oncol.* **4**, 760–768 (2003).
- O'Reilly, M. S. et al. Endostatin: an endogenous inhibitor of angiogenesis and tumor growth. *Cell* **88**, 277–285 (1997).
- Maniwa, Y., Kanki, M. & Okita, Y. Importance of the control of lung recurrence soon after surgery of pulmonary metastases. *Am. J. Surg.* **179**, 122–125 (2000).
- Lange, P. H., Hekmat, K., Bosl, G., Kennedy, B. J. & Fraley, E. E. Accelerated growth of testicular cancer after cytoreductive surgery. *Cancer* **45**, 1498–1506 (1980).
- Dromi, S. A. et al. Radiofrequency ablation induces antigen-presenting cell infiltration and amplification of weak tumor-induced immunity. *Radiology* **251**, 58–66 (2009).
- Zerbini, A. et al. Radiofrequency thermal ablation for hepatocellular carcinoma stimulates autologous NK-cell response. *Gastroenterology* **138**, 1931–1942 (2010).
- Zerbini, A. et al. Radiofrequency thermal ablation of hepatocellular carcinoma liver nodules can activate and enhance tumor-specific T-cell responses. *Cancer Res.* **66**, 1139–1146 (2006).
- Behm, B. et al. Additive antitumor response to the rabbit VX2 hepatoma by combined radio frequency ablation and toll like receptor 9 stimulation. *Gut* **65**, 134–143 (2016).
- Chu, K. F. & Dupuy, D. E. Thermal ablation of tumours: biological mechanisms and advances in therapy. *Nat. Rev. Cancer* **14**, 199–208 (2014).
- Xu, A. et al. TLR9 agonist enhances radiofrequency ablation-induced CTL responses, leading to the potent inhibition of primary tumor growth and lung metastasis. *Cell Mol. Immunol.* **16**, 820–832 (2019).
- Sanchez-Ortiz, R. F., Tannir, N., Ahrar, K. & Wood, C. G. Spontaneous regression of pulmonary metastases from renal cell carcinoma after radio frequency ablation of primary tumor: an in situ tumor vaccine? *J. Urol.* **170**, 178–179 (2003).
- Kim, H., Park, B. K. & Kim, C. K. Spontaneous regression of pulmonary and adrenal metastases following percutaneous radiofrequency ablation of a recurrent renal cell carcinoma. *Korean J. Radiol.* **9**, 470–472 (2008).
- Soanes, W. A., Ablin, R. J. & Gonder, M. J. Remission of metastatic lesions following cryosurgery in prostatic cancer: immunologic considerations. *J. Urol.* **104**, 154–159 (1970).



23. Zhou, W. et al. US-guided percutaneous microwave coagulation of small breast cancers: a clinical study. *Radiology* **263**, 364–373 (2012).
24. Burak, W. E. Jr et al. Radiofrequency ablation of invasive breast carcinoma followed by delayed surgical excision. *Cancer* **98**, 1369–1376 (2003).
25. Manenti, G. et al. Small breast cancers: in vivo percutaneous US-guided radiofrequency ablation with dedicated cool-tip radiofrequency system. *Radiology* **251**, 339–346 (2009).
26. Palussiere, J. et al. Radiofrequency ablation as a substitute for surgery in elderly patients with nonresected breast cancer: pilot study with long-term outcomes. *Radiology* **264**, 597–605 (2012).
27. Roubidoux, M. A. et al. Small (< 2.0-cm) breast cancers: mammographic and US findings at US-guided cryoablation—initial experience. *Radiology* **233**, 857–867 (2004).
28. Simon, C. J., Dupuy, D. E. & Mayo-Smith, W. W. Microwave ablation: principles and applications. *Radiographics* **25**(Suppl 1), S69–S83 (2005).
29. Zhou, W. et al. Comparison of ablation zones among different tissues using 2450-MHz cooled-shaft microwave antenna: results in ex vivo porcine models. *PLoS ONE* **8**, e71873 (2013).
30. Zhou, W. et al. Image and pathological changes after microwave ablation of breast cancer: a pilot study. *Eur. J. Radiol.* **83**, 1771–1777 (2014).
31. Li, L. et al. Microwave ablation combined with OK-432 induces Th1-type response and specific antitumor immunity in a murine model of breast cancer. *J. Transl. Med.* **15**, 23 (2017).
32. Zhu, J. et al. Enhanced antitumor efficacy through microwave ablation in combination with immune checkpoints blockade in breast cancer: a pre-clinical study in a murine model. *Diagn. Inter. Imaging* **99**, 135–142 (2018).
33. Todorova, V. K., Klimberg, V. S., Hennings, L., Kieber-Emmons, T. & Pashov, A. Immunomodulatory effects of radiofrequency ablation in a breast cancer model. *Immunol. Investig.* **39**, 74–92 (2010).
34. Danna, E. A. et al. Surgical removal of primary tumor reverses tumor-induced immunosuppression despite the presence of metastatic disease. *Cancer Res.* **64**, 2205–2211 (2004).
35. Pulaski, B. A. & Ostrand-Rosenberg, S. Reduction of established spontaneous mammary carcinoma metastases following immunotherapy with major histocompatibility complex class II and B7.1 cell-based tumor vaccines. *Cancer Res.* **58**, 1486–1493 (1998).
36. Habif, G., Crinier, A., Andre, P., Vivier, E. & Narni-Mancinelli, E. Targeting natural killer cells in solid tumors. *Cell Mol. Immunol.* **16**, 415–422 (2019).
37. Sivori, S. et al. Human NK cells: surface receptors, inhibitory checkpoints, and translational applications. *Cell Mol. Immunol.* **16**, 430–441 (2019).
38. Banh, C., Miah, S. M., Kerr, W. G. & Brossay, L. Mouse natural killer cell development and maturation are differentially regulated by SHIP-1. *Blood* **120**, 4583–4590 (2012).
39. Young, H. A. & Ortaldo, J. Cytokines as critical co-stimulatory molecules in modulating the immune response of natural killer cells. *Cell Res.* **16**, 20–24 (2006).
40. Steel, J. C., Waldmann, T. A. & Morris, J. C. Interleukin-15 biology and its therapeutic implications in cancer. *Trends Pharm. Sci.* **33**, 35–41 (2012).
41. Gerratana, L. et al. Pattern of metastasis and outcome in patients with breast cancer. *Clin. Exp. Metastasis* **32**, 125–133 (2015).
42. Gu, Y., Wu, G., Zou, X., Huang, P. & Yi, L. Prognostic value of site-specific metastases and surgery in de novo stage IV triple-negative breast cancer: a population-based analysis. *Med. Sci. Monit.* **26**, e920432 (2020).
43. Kassam, F. et al. Survival outcomes for patients with metastatic triple-negative breast cancer: implications for clinical practice and trial design. *Clin. Breast Cancer* **9**, 29–33 (2009).
44. Pulaski B. A., Ostrand-Rosenberg S. Mouse 4T1 breast tumor model. *Curr. Protoc. Immunol.* Chapter 20, Unit 20.2 (2001).
45. Ahmad, F. et al. Changes in interleukin-1beta and 6 after hepatic microwave tissue ablation compared with radiofrequency, cryotherapy and surgical resections. *Am. J. Surg.* **200**, 500–506 (2010).
46. Dong, B. W. et al. Sequential pathological and immunologic analysis of percutaneous microwave coagulation therapy of hepatocellular carcinoma. *Int. J. Hyperther.* **19**, 119–133 (2003).
47. Jansen, M. C. et al. Cryoablation induces greater inflammatory and coagulative responses than radiofrequency ablation or laser induced thermotherapy in a rat liver model. *Surgery* **147**, 686–695 (2010).
48. Chapman, W. C. et al. Hepatic cryoablation, but not radiofrequency ablation, results in lung inflammation. *Ann. Surg.* **231**, 752–761 (2000).
49. Rashid, O. M. et al. Resection of the primary tumor improves survival in metastatic breast cancer by reducing overall tumor burden. *Surgery* **153**, 771–778 (2013).
50. Vivier, E., Tomasello, E., Baratin, M., Walzer, T. & Ugolini, S. Functions of natural killer cells. *Nat. Immunol.* **9**, 503–510 (2008).
51. Gallucci, S., Lolkema, M. & Matzinger, P. Natural adjuvants: endogenous activators of dendritic cells. *Nat. Med.* **5**, 1249–1255 (1999).
52. Sauter, B. et al. Consequences of cell death: exposure to necrotic tumor cells, but not primary tissue cells or apoptotic cells, induces the maturation of immunostimulatory dendritic cells. *J. Exp. Med.* **191**, 423–434 (2000).
53. Walzer, T., Dalod, M., Robbins, S. H., Zitvogel, L. & Vivier, E. Natural-killer cells and dendritic cells: “l’union fait la force”. *Blood* **106**, 2252–2258 (2005).
54. Chavez, M. et al. Distinct immune signatures in directly treated and distant tumors result from TLR adjuvants and focal ablation. *Theranostics* **8**, 3611–3628 (2018).
55. Kuniwa, T. et al. NK cells activated by Interleukin-4 in cooperation with Interleukin-15 exhibit distinctive characteristics. *Proc. Natl Acad. Sci. USA* **113**, 10139–10144 (2016).
56. Zhang, M. et al. IL-15 enhanced antibody-dependent cellular cytotoxicity mediated by NK cells and macrophages. *Proc. Natl Acad. Sci. USA* **115**, E10915–E10924 (2018).
57. Yoshimoto, T. et al. IL-12 up-regulates IL-18 receptor expression on T cells, Th1 cells, and B cells: synergism with IL-18 for IFN-gamma production. *J. Immunol.* **161**, 3400–3407 (1998).
58. Malek, T. R., Yu, A., Scibelli, P., Lichtenheld, M. G. & Codias, E. K. Broad programming by IL-2 receptor signaling for extended growth to multiple cytokines and functional maturation of antigen-activated T cells. *J. Immunol.* **166**, 1675–1683 (2001).